DTIC FILE COPY

AD-A199 698

DTIC ELECTE SEP 27 1988 H

REPORT DOCUMENTATION PAGE

1b. RESTRICTIVE MARKINGS —	
2a. SECURITY CLASSIFICATION AUTHORITY —	3. DISTRIBUTION / AVAILABILITY OF REPORT Approved for public release and sale; its distribution is unlimited.
2b. DECLASSIFICATION / DOWNGRADING SCHEDULE —	
4. PERFORMING ORGANIZATION REPORT NUMBER(S) Technical Report No. 65	5. MONITORING ORGANIZATION REPORT NUMBER(S) —
6a. NAME OF PERFORMING ORGANIZATION Case Western Reserve University	6b. OFFICE SYMBOL (If applicable) —
6c. ADDRESS (City, State, and ZIP Code) Cleveland, Ohio 44106	7a. NAME OF MONITORING ORGANIZATION ONR Chemistry Program
8a. NAME OF FUNDING / SPONSORING ORGANIZATION Office of Naval Research	8b. OFFICE SYMBOL (If applicable)
8c. ADDRESS (City, State, and ZIP Code) Arlington, Virginia 22217-5000	7b. ADDRESS (City, State, and ZIP Code) Arlington, Virginia 22217-5000
	9. PROCUREMENT INSTRUMENT IDENTIFICATION NUMBER Contract No. N00014-83-K-0343
	10. SOURCE OF FUNDING NUMBERS: PROGRAM ELEMENT NO. — / PROJECT NO. NR359 451 / TASK NO. — / WORK UNIT ACCESSION NO —

11. TITLE (Include Security Classification)
Electrochemistry of Carbon Relative to Batteries and Fuel Cells

12. PERSONAL AUTHOR(S)
Ernest Yeager and Donald Tryk

13a. TYPE OF REPORT	13b. TIME COVERED	14. DATE OF REPORT (Year, Month, Day)	15. PAGE COUNT
Technical Report	FROM 1987 TO 1988	September 1, 1988	15

16. SUPPLEMENTARY NOTATION
To be published in the Proceedings of the 33rd International Power Sources Symposium

17. COSATI CODES			18. SUBJECT TERMS (Continue on reverse if necessary and identify by block number)
FIELD	GROUP	SUB-GROUP	carbon, graphite, electrochemical properties, modified carbon surfaces.

19. ABSTRACT (Continue on reverse if necessary and identify by block number)

Carbon of various types are extensively used in battery and fuel cell applications as an electronic conductor, a catalyst for specific reactions, a support for other catalysts and as a high surface area electrode affording a large total capacity (capacitor batteries). This report considers the basic properties of carbons and graphites of importance to these applications including

- the electronic and solid state properties;
- pore structure of activated carbons;
- intrinsic surface electronic and electrochemical properties;
- surface chemical groups and acid/base properties;
- redox reactions on carbon and graphite surfaces;
- electrocatalytic properties of carbon surfaces for various electrode reactions;
- chemically modified carbon/graphite surfaces;
- electrochemical oxidation of carbon in battery and fuel cell applications.

20. DISTRIBUTION / AVAILABILITY OF ABSTRACT	21. ABSTRACT SECURITY CLASSIFICATION
☒ UNCLASSIFIED/UNLIMITED ☐ SAME AS RPT ☐ DTIC USERS	unclassified
22a. NAME OF RESPONSIBLE INDIVIDUAL Ernest B. Yeager, Professor of Chemistry	22b. TELEPHONE (Include Area Code) (216) 368-3626 / 22c. OFFICE SYMBOL —

DD FORM 1473, 84 MAR — 83 APR edition may be used until exhausted. All other editions are obsolete.

SECURITY CLASSIFICATION OF THIS PAGE
UNCLASSIFIED

88 9 26 08

OFFICE OF NAVAL RESEARCH

Research Contract N00014-83-K-0343

Project NR 359-451

TECHNICAL REPORT NO. 65

ELECTROCHEMISTRY OF CARBON RELATIVE TO BATTERIES AND FUEL CELLS

by

Ernest Yeager and Donald Tryk

Submitted for Publication

in

Proceedings of the
33rd International Power Sources Symposium
Cherry Hill, New Jersey
June 13-16, 1988

Case Center for Electrochemical Sciences
and the Department of Chemistry
Case Western Reserve University
Cleveland, Ohio 44106

September 1, 1988

Presented at the 33rd International Power Sources Symposium,
Cherry Hill, New Jersey, on 13-16 June 1988:

ELECTROCHEMISTRY OF CARBON RELATIVE TO BATTERIES AND FUEL CELLS

by

Ernest Yeager and Donald Tryk
Case Center for Electrochemical Sciences
and the Chemistry Department
Case Western Reserve University
Cleveland, Ohio 44106

I. INTRODUCTION

Carbon occupies a position of unusual importance to batteries and fuel cells. Its functions in such energy conversion devices are summarized in Table 1. The incorporation of carbon or graphite in an oxide positive electrode can insure good electronic conductivity in the electrode phase when it is deeply discharged, even if the higher and/or lower valency states are not good electronic conductors (e.g., the MnO_2 cathode, which has metal-like electronic conductivity in the Mn(IV) state but is an insulator in the lower valency states). The pores within the carbon electrode also can store reactants, products and intermediates. An illustration of such is the Teflon-bonded porous carbon electrode used as the cathode in oxyhalide cells in which the solid LiCl produced at the cathode is stored within the electrolyte-filled pores. The pore structure in the carbon may also play a role in gas transport within Teflon-bonded porous electrodes. The carbon surface may serve as a catalyst for such reactions as O_2 reduction in metal-air batteries and the reduction of thionyl chloride in lithium-oxyhalide batteries. In some of the capacitor batteries, high area activated carbons are used to achieve very high electrolytic capacitance. This capacitance may be associated with the ionic double layer (non-Faradaic charge) or with changes in the oxidation states of functional groups attached to the carbon surface (Faradaic charge).

II. STRUCTURAL CONSIDERATIONS

Graphite: The crystal structure of graphite is shown in Fig. 1. Graphite is unique among the materials used as electrode surfaces in that all of the valency forces for the basal plane are satisfied in the plane of the surface. The edge surfaces, however, bristle with functional groups and thus have very different chemical and electrochemical behavior.

The electrochemical behavior of single crystal graphite (particularly the basal plane) is approximated by highly ordered pyrolytic graphite (HOPG), prepared by stress-annealing ordinary pyro-

lytic graphite at high temperatures (3000°C) and pressures (15 kbars). The double layer capacitance of the basal plane of HOPG is plotted as a function of electrode potential in Fig. 2 (1). The basal plane surface was prepared by peeling off a layer of the graphite by means of a piece of adhesive tape. The capacitance is remarkably small and parabolically dependent on potential rather than the usual hyperbolic dependence of a semiconductor. Furthermore, in contrast to metal electrodes, the capacitance is not pH-dependent and is not affected by the addition of iodide anions, indicating that the iodide ion does not adsorb on the basal plane.

The parabolic dependence of the capacitance has been explained by Gerischer (2,3) on the basis of the low density of electronic states in graphite at and near the Fermi level (see Fig. 3). This low density is the result of the small or negligible overlap of the valence and conduction bands (see Fig. 3b). The result is a substantial potential drop across a space charge region within the graphite perpendicular to the basal plane. Qualitatively, this situation is as shown in Fig. 4 with the electric field penetrating several Angstroms into the graphite, compared with a fraction of an Angstrom (Fermi screening distance) for a metal such as copper.

The space charge region in the graphite has associated with it a capacitance C_{sc} (see Fig. 5) which is in series with the usual diffuse layer (C_{diff}) and Helmholtz layer (C_H) capacitances. Since $C_{sc} < C_H < C_{diff}$, the capacitance behavior of the interface is predominated by C_{sc}. This results in the behavior in Fig. 3.

The kinetics of simple redox reactions such as:

$$Fe(CN)_6^{3-} + e^- = Fe(CN)_6^{4-} \qquad (1)$$

are substantially slower on the basal plane of HOPG than on the polished edge surface (5). Rotating disk electrodes (Fig. 6) indicate that the standard electron transfer rate constant for reaction 1 is several times greater on the edge surface ($k^o = 6.2 \times 10^{-3}$ cm s^{-1}) than on the cleaved basal plane ($k^o = 2.3 \times 10^{-3}$ cm s^{-1}). The lower k^o on the basal plane may reflect the anisotropic space charge region in the graphite but other factors may contribute, including differences in the potential of zero charge and differences in the true surface areas. The true surface area for the edge orientation is probably considerably higher than on the HOPG basal plane. When the edge surface is polished, the situation is rather analogous to polishing the edges of a book. The layers of the HOPG structures are bent over so as to expose principally the basal plane.

The electron transfer rate constants for the $Fe(CN)_6^{3-}/Fe(CN)_6^{4-}$ couple on the basal and edge planes are at least several orders of magnitude lower than on gold in K^+ containing electrolytes (6). In good part this large difference is probably caused by the potential

drop across the space charge region in the graphite.

The hydrogen overpotential is quite high on both the basal plane and polished edge plane of HOPG as evidenced from the linear sweep voltammetry curves in Fig. 7 (7). At a current density of ~ 5 x 10^{-4} A/cm^2, the hydrogen overpotential on both surfaces is ~ -0.9 V in 1 M H_2SO_4. The O_2 overpotential is also moderately high (~ +0.8 V) on the basis of Fig. 7. The anodic current at the limit of the anodic sweep, however, also includes the electroxidation of the graphite.

Intercalation of the HOPG occurs at very anodic and cathodic potentials (8,9). At the former, the graphite is oxidized through the loss of electrons from the valence band and the penetration of an anion between the planes to compensate the positive charge as shown in Fig. 8. An analogous situation occurs for the reduction with the charge compensation by the cation.

Carbon Blacks: The several states of aggregation involved in a carbon black are shown in Fig. 9 (10). The primary structural units are two-dimensional polyacene platelets, consisting of 40 to 100 fused rings with various edge functional groups (see Fig. 9a). Three to five of these platelets are organized in platelet bundles. One hundred to 1,000 of these platelets are in turn in nodules with crystallite properties. These nodules are in aggregates as shown in Fig. 9c. With non-activated carbon blacks, the nodules are relatively non-porous and the surface area as measured by BET adsorption is essentially that of the outside surface of the nodules. With activation through partial oxidation with an oxidizing agent such as steam, micropore structure is developed within the nodules and the surface area is greatly increased (e.g., from 60 m^2/g to 200 m^2/g for steam-activated acetylene black).

Some properties are listed in Table 2 for high surface area carbons used in fuel cell and metal-air battery applications. With the exception of the Shawinigan black, all of the carbons in Table 2 involve particles or nodules with internal surface areas. With extremely high surface area furnace blacks such as Black Pearls, the area is too high to explain in terms of capillaries or well defined pores. The walls would be only a few Angstroms thick. It is probably better to view such activated carbon particles as more like balls of twine.

III. CARBON ELECTROCHEMICAL OXIDATION

Under the conditions prevailing in air cathodes in fuel cells and metal-air batteries, as well as battery oxide positive electrodes, carbon would be expected to oxidize on the basis of thermodynamic considerations. The oxidation reactions to form CO and CO_2 and the corresponding thermodynamic standard electrode potentials are as follows (11):

$$C + H_2O \rightarrow CO + 2H^+ + 2e^-;\ E^\circ = +0.548\ V \quad (2)$$

$$C + 2H_2O \rightarrow CO_2 + 4H^+ + 4e^-;\ E^\circ = +0.207\ V \quad (3)$$

where the standard electrode potentials are at 25°C versus the NHE. In practice, these oxidation reactions are kinetically very inhibited and the oxidation rates are strongly dependent on the type of carbon as well as its surface area, with order of magnitude differences in oxidation rates between various carbons (12-15). In general, the more graphitized the carbon structure is, the lower is the oxidation rate. For air cathodes in alkaline and acid fuel cells and particularly bifunctional O_2 electrodes in rechargeable air cells, the oxidation of the carbon substrate structure sets a limit on the useful life.

The current associated with the oxidation of a Shawinigan black in a fuel cell-type Teflon-bonded carbon air electrode (without added catalysts) is shown in Fig. 10. The current is only semiquantitatively related to the carbon oxidation rate since the oxidation reaction can yield products corresponding to only partial oxidation. At +0.50 V vs. Hg/HgO, OH^- in 4 M KOH at 25°C, the oxidation current corresponds to a loss of 30 percent of the carbon in 2000 h. With a catalyst such as highly dispersed Pt, the carbon oxidation may be accelerated as the Pt acts as an oxidation catalyst and literally burns holes in the carbon support where the Pt particles sit (17). This is one of the main reasons why fuel cell electrochemists are seeking new supports such as stable electronic conducting oxides as replacements for high area carbons.

IV. SURFACE CHEMISTRY OF CARBON AND O_2 ELECTROCATALYSIS

Some of the surface groups which are proposed to be present on the edges of the platelet are shown in Fig. 11. These functional groups can impart catalytic properties to carbon electrodes. For example, O_2 reduction proceeds readily to hydrogen peroxide in alkaline solutions according to the reaction:

$$O_2 + H_2O + 2e^- = HO_2^- + OH^- \quad (4)$$

on ordinary carbon surfaces and the edge surface of the HOPG but is very inhibited on the basal place of HOPG (5). This has been explained on the basis that rection 4 is catalyzed by quinoid groups present on most carbon surfaces but missing on the basal plane of HOPG (19-22). To test this hypothesis, such quinones as 9,10-phenanthrenequinone and naphthoquinone have been pre-adsorbed on the basal plane of HOPG (21,22). The O_2 reduction to peroxide is then no longer inhibited on this surface, confirming the catalytic role of the quinones. Anthraquinones chemically bound to the graphite surface through an amide linkage also appear to promote reaction 4.

Various mechanisms by which the quinones promote reaction 4 have been proposed. The redox properties of the quinone/semiquinone couple appear to be important (19,21). One mechanism proposed by Garten and Weiss (19) is shown in Fig. 12.

With high area carbon gas-fed air cathodes in alkaline solutions, the O_2 reduction proceeds with fast kinetics to the peroxide. The further reduction of peroxide

$$HO_2^- + H_2O + 2e^- \rightarrow 3OH^- \quad (5)$$

or decomposition

$$2HO_2^- \rightarrow O_2 + 2OH^- \quad (6)$$

is essential for a high performance air cathode from the standpoint of both low polarization and long operating life. The reduction and decomposition reactions are slow on carbon and graphite even with trace transition metals present. Consequently, a peroxide decomposition catalyst is usually added, such as a transition metal macrocycle or a transition metal oxide. The overall reaction via either reactions 4 + 5 or 4 + 6 is then the 4-electron reduction to OH^-

$$O_2 + 2H_2O + 4e^- \rightarrow 4OH^- \quad (7)$$

When a very active catalyst for the overall 4-electron process, such as highly dispersed platinum, is introduced into the porous carbon electrode, the overall direct 4-electron reduction pathway may become predominant.

Excellent performance at very high current densities can be obtained with O_2 cathodes using a peroxide decomposition catalyst and relying on the high area carbon to promote the O_2 reduction to the peroxide via reaction 4. Particularly effective peroxide elimination catalysts are the heat-treated transition metal macrocycles such as the cobalt-ms-tetra-p-methoxy phenyl porphyrin (Co-TMPP) (Fig. 13). Such species are strongly adsorbed on high area carbon surfaces but generally lack the long term stability needed for most fuel cell and air battery applications. If such macrocycles, adsorbed at monolayer levels on high area carbons, are heat treated at 450 to 800°C, the macrocycles undergo partial decomposition but appear to bind chemically to the carbon surface (22,23). EXAFS measurements on the heat-treated Co-TMPP carried out by McBreen and O'Grady (24) at Brookhaven as well as Scherson and Bae (25) of Case Western Reserve University provide evidence that a significant fraction of the N_4 centers are still intact. These function as binding sites for the Co, which then serves as the peroxide decomposition catalyst. Nitrogen binding sites for transition metals with less than four nitrogens may also be present after the heat treatment but the N_4 sites probably bind the

transition metal most strongly. Mass spectroscopic studies of the gaseous products produced during the heat treatment indicate that the nitrogen is not lost from the surface (26).

A typical polarization curve for O_2 reduction using the heat-treated Co-TMPP/carbon catalyst is shown in Fig. 14. The $NaOH/NaAl(OH)_4$ electrolyte corresponds to that which may be used in an aluminum-air battery. The linear Tafel behavior with a slope of ~-0.03 V/decade over three decades fits the peroxide pathway with fast kinetics for reaction 4, and reaction 6 the rate determining step. On air, mass transport of O_2 sets the upper limit.

In concentrated alkaline solutions, O_2 is also reduced to the superoxide anion; i.e.,

$$O_2 + e^- \rightarrow O_2^- \qquad (8)$$

This corresponds to an outer sphere electron transfer with the electron tunnelling between electron orbitals at and near the Fermi level in the carbon or graphite and the partially occupied π^* orbitals of the O_2 molecules. The superoxide radical anion O_2^- is then decomposed via the homogeneous reaction

$$2O_2^- + H_2O = O_2 + HO_2^- + OH^- \qquad (9)$$

In aqueous solutions reaction 8 is relatively slow and O_2 reduction to O_2^- via reaction 8 represents only a small fraction of the total reduction current (28). In aprotic solvents such as acetonitrile, however, O_2 reduction to the O_2^- is predominant on graphite electrodes (including the basal plane) in electrolytes not involving a strong Lewis acid but instead a salt such as the tetraalkyl ammonium perchlorate (21,29).

V. CARBON CATHODES IN OXYHALIDE BATTERIES

Important factors involved in optimizing Teflon-bonded porous carbon cathodes for oxyhalide batteries include the following:

1. Void volume

The reduction reaction for thionyl chloride may be written as

$$4Li + 2SOCl_2 \rightarrow 4LiCl + S + SO_2 \qquad (10)$$

The LiCl has very limited solubility in $SOCl_2$ and precipitates within the carbon pore structures (30). To maximize the half-cell discharge capacity, the void volume in the porous carbon electrode should be as large as possible while still providing adequate electronic conductivity. The void volume can be increased to greater than 85% by using carbon blacks with agglomerate structures with the nodules

strung together in open networks. The pore void volume can also be increased by the use of a pore former (31) such as NH_4HCO_3 which is volatilized out of the carbon electrode during the heat treatment used to promote sintering of the Teflon binder.

2. Catalytic aspects

The catalytic activity of carbons for the reduction of oxyhalide solvents is not well established. Klinedinst (31) has studied the performance characteristics of various high area carbons in oxyhalide cathodes and found the overpotential for $SOCl_2$ reduction to be essentially independent of the surface area for carbon blacks with 250 m^2/g and higher. Similar overpotentials to those obtained with a high area carbon can be obtained with a low area carbon by using a catalyst such as dispersed platinum.

In studies of sulfuryl chloride cells, Walker et al. (32) have found that both the cathode potential at high current densities and the charge capacity for carbon blacks such as Shawinigan acetylene black and Cabot Black Pearls 2000 can be greatly improved by treating the carbon with acetone in the presence of $KMnO_4$ and KOH prior to electrode fabrication. This treatment produces no change in the surface area of the Shawinigan black but increases the total pore volume by more than 2-fold. The acetone-water solution after this treatment was found to yield a fluffy white solid containing Ca and S. Walker et al. (32) suggest that $CaCl_2$ precipitation in the pores of the untreated carbon black blocks the pores. There is no evidence for a change in the catalytic activity of the carbon surface after the acetone treatment, although such is possible.

Various catalysts have been added to the carbon cathodes used in oxyhalide batteries, including dispersed platinum, gold, nickel oxide and copper (30,33). Kinoshita has reviewed the various catalysts used with carbon cathodes in oxyhalide batteries (34). Doddapaneni (35) has reported that the Co and Fe phthalocyanines catalyze the reduction of $SOCl_2$. With very high area carbons (>250 m^2/g), however, it is not clear whether these various catalysts add very much to the overall intrinsic activity of the carbon surface. Instead, their principal effect may be to change the distribution of the lithium chloride and other insoluble discharge products in the carbon cathodes (30).

The oxyhalide reduction reactions are not well understood, particularly the electrocatalytic-mechanistic aspect, and further basic research is needed. Various in situ spectroscopic techniques are promising for such studies.

Acknowledgments: Some of the experimental results presented in this paper are based on research sponsored by the U.S. Office of Naval Research and the Department of Energy.

REFERENCES

1. J. P. Randin and E. Yeager, J. Electroanal. Chem., 36, 257 (1972).

2. H. Gerischer, J. Phys. Chem., 89, 4249 (1985).

3. H. Gerischer, R. McIntyre, D. Scherson and W. Storck, J. Phys. Chem., 91, 1930 (1987).

4. I. L. Spain, in "Chemistry and Physics of Carbon," Vol. 16, P. L. Walker, Jr. and P. A. Thrower, Editors, pp. 119-304, Marcel Dekker, New York (1981).

5. I. Morcos and E. Yeager, Electrochim. Acta, 15, 953 (1970).

6. J. Kuta and E. Yeager, J. Electroanal. Chem., 59, 110 (1975) and L. M. Peter, W. Durr, P Bindra and H. Gerischer, J. Electroanal. Chem., 71, 31 (1976).

7. J. Kuta and E. Yeager, unpublished research, as quoted in E. Yeager, J. Molla and S. Gupta, in "The Electrochemistry of Carbon," S. Sarangapani, J. R. Akridge and B. Schumm, Editors, pp. 123-157, The Electrochemical Society, Pennington, NJ (1984).

8. A. W. Moore, in "Chemistry and Physics of Carbon," Vol. 17, P. L. Walker, Jr. and P. A. Thrower, Editors, pp. 233-286, Marcel Dekker, New York (1981).

9. F. Beck and H. Krohn, in Ref. 7, pp. 574-594.

10. T. J. Fabish and D. E. Schleifer, in Ref. 7, pp. 79-109.

11. J. Van Muylder and M. Pourbaix, in "Atlas of Electrochemical Equilibria in Aqueous Solutions," M. Pourbaix, Editor, pp. 449-457, Pergamon, Oxford (1966).

12. K. Kinoshita and J. A. S. Bett, in "Corrosion Problems in Energy Conversion and Generation," C. S. Tedmon, Editor, pp. 43-55, The Electrochemical Society, Pennington, NJ (1974).

13. P. Stonehart, Carbon, 22, 423 (1984).

14. P. N. Ross and M. Sattler, J. Electrochem. Soc., 135, 1464 (1988).

15. D. Tryk, W. Aldred and E. Yeager, in Ref. 7, pp. 192-220.

16. D. Tryk, W. Aldred and E. Yeager, "Bifunctional Oxygen Electrodes," UCRL-15549, final report, October 1980 - April 1983, prepared by Case Western Reserve University for Lawrence Livermore Laboratory, U.S. Department of Energy Subcontract No. 1377901 (1983).

17. L. Gestaut, J. C. Huang, T. M. Clere, L. A. Knerr, W. R. Bennett, A. L. Barnes and D. J. Wheeler, in Ref. 7, pp. 344-362. See also discussion in K. Kinoshita, "Carbon: Electrochemical and Physicochemical Properties," pp. 316-337, Wiley, New York (1988).

18. J. S. Mattson and H. B. Mark, Jr., "Activated Carbon," Marcel Dekker, New York, p. 39 (1971).

19. V. A. Garten and D. E. Weiss, Aust. J. Chem., 8, 68 (1955).

20. Z. W. Zhang, D. Tryk and E. Yeager, in Ref. 7, pp. 158-178.

21. M. S. Hossain, Ph.D. Dissertation, Case Western Reserve University, 1986.

22. E. Yeager, J. Mol. Catal., 38, 5 (1986).

23. A. A. Tanaka, Ph.D. Dissertation, Case Western Reserve University, 1987.

24. J. McBreen, W. E. O'Grady, D. E. Sayers and C. Y. Yang in "Extended Abstracts," Vol. 8-71, p. 146, The Electrochemical Society, Pennington, NJ (1987).

25. D. Scherson and I. Bae, unpublished results.

26. D. Scherson, A. A. Tanaka, S. L. Gupta, D. Tryk, C. Fierro, R. Holze, E. B. Yeager and R. P. Lattimer, Electrochim. Acta, 31, 1247 (1986).

27. E. B. Yeager, D. Tryk, S. L. Gupta and W. Aldred, in "Aluminum-Air Battery Development," final report, January 1984 - June 1986, prepared by Eltech Systems Corporation for Lawrence Livermore Laboratory, U.S. Department of Energy Contract No. 1806205 (1987).

28. J. Lu, D. Tryk and E. Yeager, in "Extended Abstracts," Vol. 82-2, pp. 520-521, The Electrochemical Society, Pennington, NJ (1982).

29. K. A. Radyushkina, E. O. Zonina and and M. R. Tarasevich, Elektrokhim., 20, 977 (1984).

30. C. R. Schlaikjer, in "Lithium Batteries," J. P. Gabano, Editor, pp. 329-330, Academic, New York (1983).

31. K. A. Klindinst, J. Electrochem. Soc., 132, 2044 (1985).

32. C. W. Walker, Jr., M. Binder, W. L. Wade, Jr. and S. Gilman, J. Electrochem. Soc., 132, 1536 (1985).

33. K. Klinedinst and F. G. Murphy, German Patent 2,951,167, July 10, 1980.

34. K. Kinoshita, "Carbon: Electrochemical and Physicochemical Properties," pp. 421-427, 504-505, Wiley, New York (1988).

35. N. Doddapeneni, in "Extended Abstracts," Vol. 81-1, pp. 218-219, The Electrochemical Society, Pennington, NJ (1981).

36. S. B. Seeley, in "Kirk-Othmer Encyclopedia of Chemical Technology," 3rd Edition, Vol. 4, p. 691, Wiley, New York (1978).

Table 1.

FUNCTIONS OF CARBON/GRAPHITE IN BATTERY ELECTRODES

- Electronic Conductor
- Pore Structure
  - Storage, retention of reactants, products
  - Mass transport system
- Electrocatalysis
  - Intrinsic catalytic properties
  - Chemically modified surfaces
  - Catalyst support
- Heat Transfer
- Electrolytic Capacitance
  - Double layer
  - Faradaic

TABLE 2

PHYSICAL AND CHEMICAL PROPERTIES OF VARIOUS CARBONS[A]

TYPE OF CARBON (MANUFACTURER)	SOURCE	SURFACE AREA (BET) $M^2 G^{-1}$	MEAN PARTICLE SIZE, NM	ASH CONTENT %	FE CONTENT %
SHAWINIGAN BLACK (GULF)	THERMAL DECOMPOSITION ACETYLENE	67	42	0.05	0.002
VULCAN XC-72 (CABOT)	FURNACE PROCESS CARBON BLACK	250	30	2.0	(0.1)[B]
KETJEN BLACK (AKMAK)	NATURAL GAS PETROLEUM DISTILLATES AND RESIDUES	950	30	0.5	—
RB CARBON (CALGON)	BITUMINOUS COAL	1150-1350	65-75% <44μM	23	1.57
DE ASHED RB CARBON (EMC)	"	1583	"	~2	(0.31)[B]
P 55 (USSR)	CHARCOAL	1000	—	—	(0.74)[B]
BLACK PEARLS	FURNACE BLACK	1500	15	—	—

[A]DATA PROVIDED BY MANUFACTURER UNLESS OTHERWISE INDICATED.

[B]VALUES IN PARENTHESES WERE DETERMINED BY INDEPENDENT ANALYTICAL LABORATORIES.

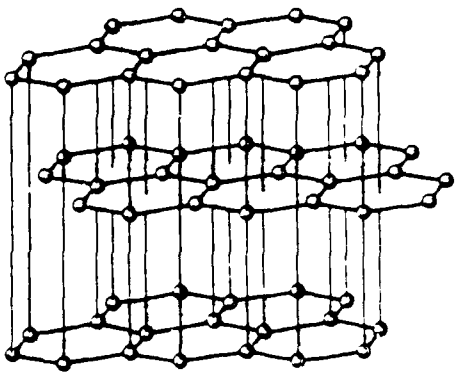

Fig. 1. Hexagonal Structure of Graphite (after Ref. 36).

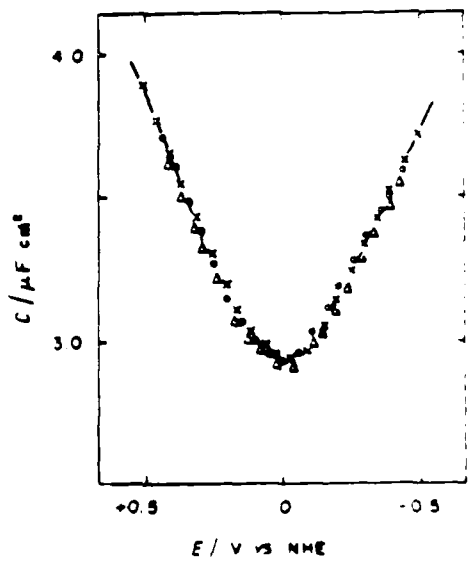

Fig. 2. Capacity curves [illegible] stress-annealed pyrolytic graphite [illegible] = 0.4°] in NaF + NaI solutions [illegible] at 25°C and 1 kHz (Teflon hood [illegible] peeled off dry) (1) [illegible] (X) [illegible] M NaF + 0.1 M NaI; (Δ) [illegible] M NaF + [illegible] M NaI.

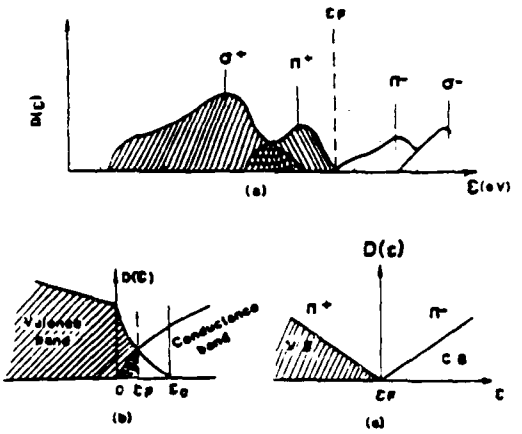

Fig. 3 (a) Sketch of the density of states for graphite. Zero energy is taken at the vacuum level. (b) Density of states for 3D graphite near the region of band overlap. Zero energy is taken at the bottom of the conduction band. (c) Density of states for a single sheet of carbon atoms (2D graphite) near the band-touching region (4).

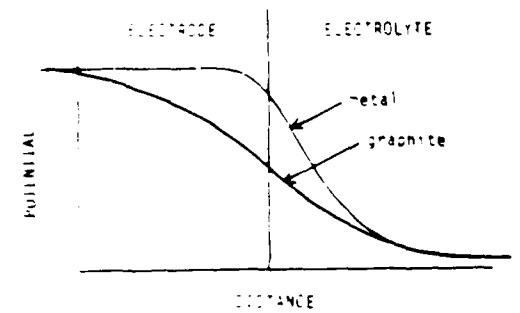

Fig. 4. Potential distribution across metal-electrolyte and graphite-electrolyte interfaces.

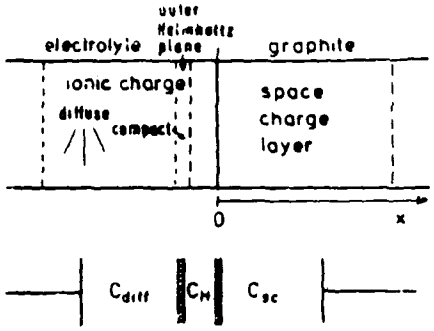

Fig. 5. The graphite-electrolyte interface (8).

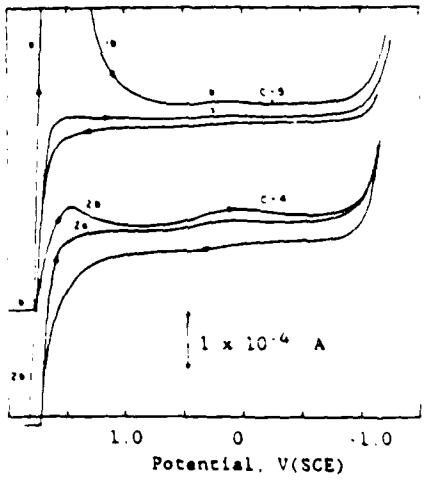

Fig. 7. Oxygen and hydrogen evolution on pyrolytic graphite. (1) electrode C-5 (edge plane, polished); (2) electrode C-4 (basal plane). Electrolyte: 1 M H_2SO_4; electrode area: 0.196 cm^2; rotation rate: 3600 rpm; scan rate: 4 V/min. Direction of sweep indicated by arrows. (Curves a and b differ in range of potentials of scans) (7).

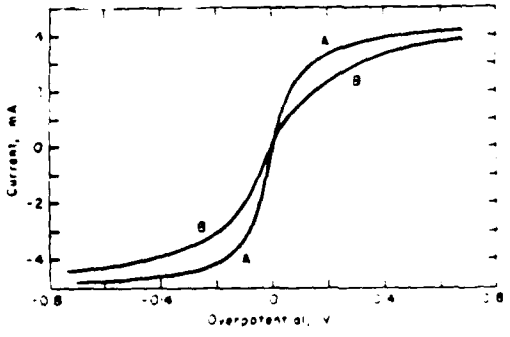

Fig. 6. Overpotential curves for the ferri-ferrocyanide couple on high pressure annealed pyrolytic graphite. Solution: 0.005 M $K_3Fe(CN)_6$ + 0.005 M $K_4Fe(CN)_6$ + 0.5 M K_2SO_4 adjusted to pH 3; temperature, 26°C; rotation rate, 3920 rpm. A, edge surface. B, cleavage surface.

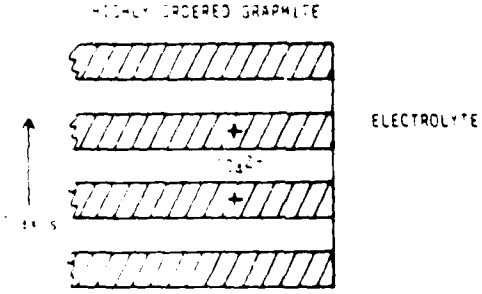

Fig. 8. Intercalation of highly ordered pyrolytic graphite.

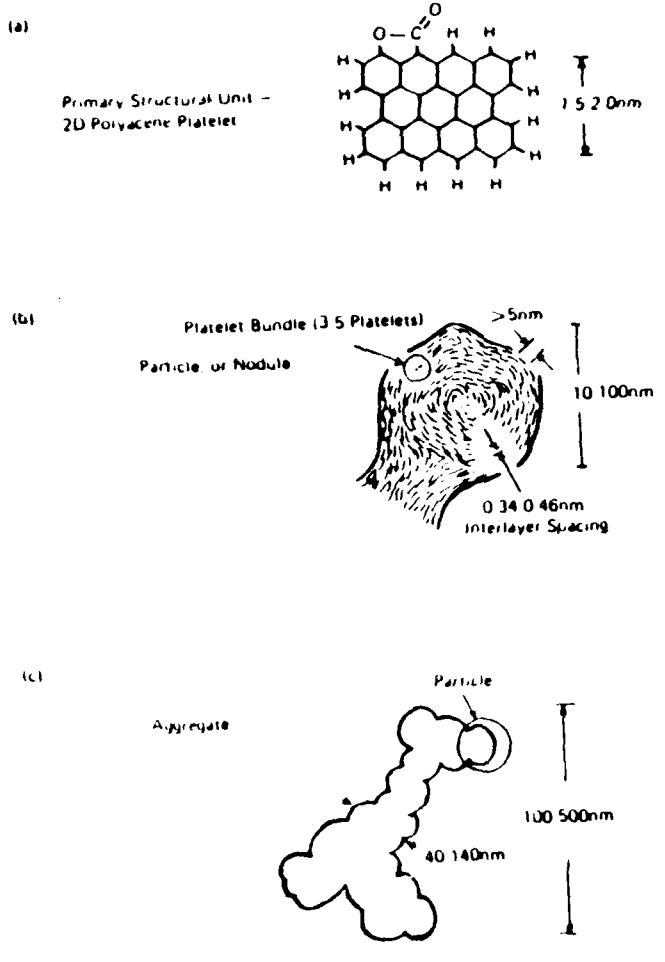

Fig. 9 Structural units of carbon black (10): (a) two dimensional platelets (40-100 fused rings), (b) nodule (100-1000 platelets) in crystallites; (c) aggregate (100-1000 nodules)

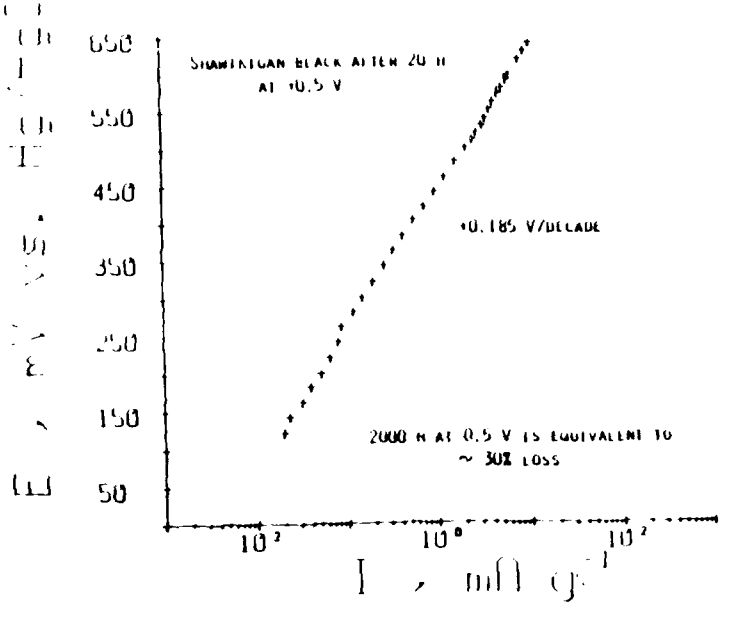

Fig. 10. Anodic polarization curve for Shawinigan Black (100 mg) + Teflon T30B (20 mg) electrode (2.4 cm^2) in N_2-saturated 4 M KOH at 25°C (16).

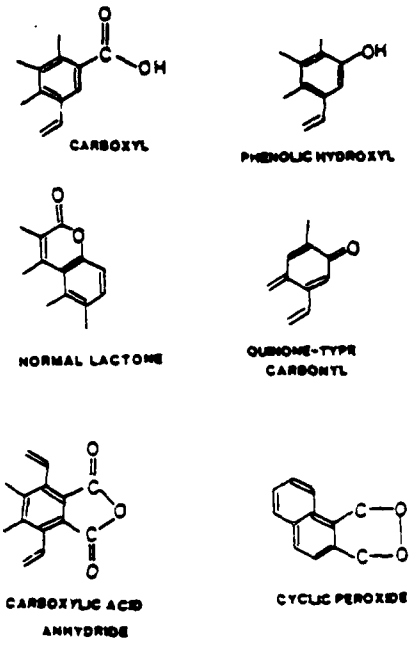

Fig. 11. Proposed functional groups on carbon surfaces (after Ref. 22)

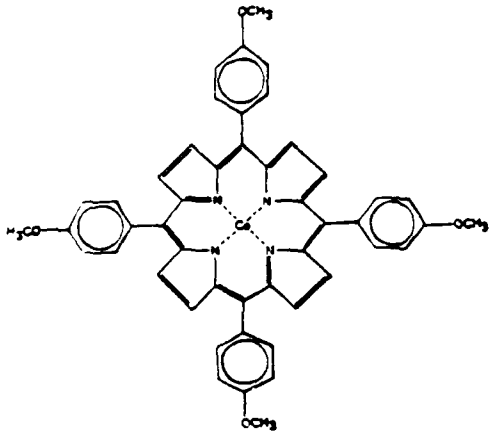

Fig. 13. Cobalt-ms-tetra-p-methoxy phenyl porphyrin (Co-TMPP).

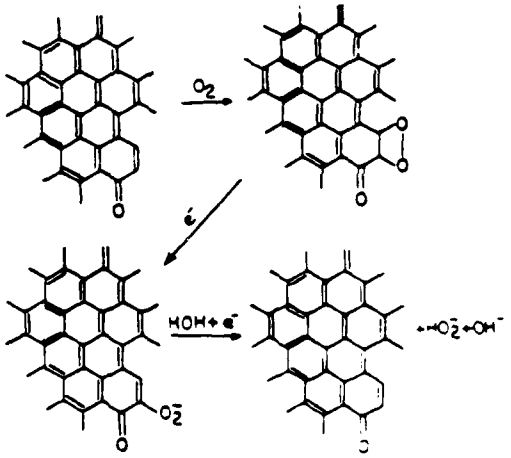

Fig. 12. Garten and Weiss mechanism for O_2 reduction on carbon surfaces [23]

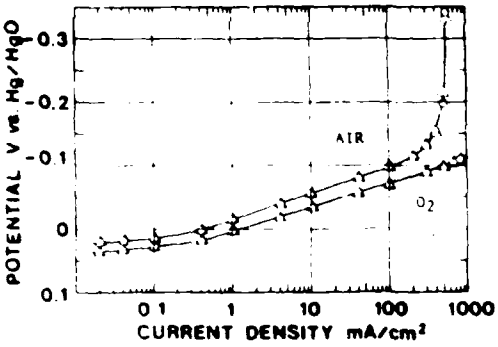

Fig. 14. Polarization curves for O_2 reduction with gas-fed (1 atm) electrodes at 60°C in (○) 4 M NaOH and (△) 4 M NaOH + 1 M $NaAl(OH)_4$. Active layer contained 14.6 mg cm^{-2} CoTMPP/XC-72 (4.8% wt %, 450°C HT) and 6.2 mg cm^{-2} Teflon T30B. Teflon-bonded material was heat-treated at 280°C in flowing He for 2 h. Teflon/C hydrophobic backing with Ag-plated Ni screen (EMC Corp.) was used [27].